*Sensors and Materials*, Vol. 28, No. 1 (2016) 55–60
MYU Tokyo



S & M 1156

# Correction of Mass Effect of Nonelectroded Region of a Quartz Crystal Microbalance (QCM) in Ultra-Micromass Measurement

Wei Fu, Qingsong Bai, and Xianhe Huang*

University of Electronic Science and Technology of China, Chengdu 611731, China

(Received June 25, 2015; accepted September 8, 2015)

***Keywords:*** mass effect of nonelectroded region, QCM, correction

When applying a quartz crystal microbalance (QCM) to ultra-micromass measurement, not only the electroded region but also the nonelectroded region absorb analytes. The mass loading on the sensing surface of the QCM chip (with both electroded and nonelectroded regions) causes a shift in the frequency of the QCM. A method based on the integral of the mass sensitivity function is presented in this paper which can distinguish between the frequency shift caused by the electroded region and that caused by the nonelectroded region. Finally, the feasibility of the correction method can be confirmed on the basis of the data processing results of an airborne Vaccinia virus testing experiment using a QCM.

## 1. Introduction

Many important physical and chemical processes can be observed through associated mass changes. A quartz crystal microbalance (QCM) is a simple, rapid, and high-resolution mass-sensing device. Application of the QCM have a bright future because its unique merits include high sensitivity, response to a broad spectrum, simplicity of operation, real-time output, and label-free analysis.[1] The linear relationship between the adsorption of mass and the frequency shift can be described using Sauerbrey's equation[2]

$$\Delta m = -\frac{\rho_q \times t_q}{f_0} \times \Delta f = -C_{QCM} \times \Delta f, \tag{1}$$

where $\rho_q$ and $t_q$ are the density and thickness of the quartz plate, and $\Delta m$ and $\Delta f$ are the mass change and frequency shift, respectively; $f_0$ is the operating frequency of the QCM, and $C_{QCM}$ is the mass sensitivity constant. For a 5 MHz AT-cut crystal, $C_{QCM}$ =17.7 ng·cm$^{-2}$Hz$^{-1}$, whereas for a 5 MHz 3rd overtone AT-cut crystal, $C_{QCM}$ = 53.1 ng·cm$^{-2}$Hz$^{-1}$.

The sensing surface of a QCM is usually divided into an electroded region and a nonelectroded region. A large number of QCM experiments have proven that a mass change in the entire area of the electroded and nonelectroded area causes a shfit in the frequency of the resonator. In a practical application, analytes will not only be adsorbed onto the electroded region but also onto the nonelectroded region. To satisfy the energy trapping condition, the area of the nonelectroded

*Corresponding author: e-mail: xianhehuang@uestc.edu.cn

ISSN 0914-4935 © MYU K.K.

region on the crystal plate must be larger than that of the electroded region. On the other hand, according to the energy trapping theory, the energy of the vibration wave of the crystal resonator decreases exponentially as the propagation distance increases. Thus the mass sensitivity rapidly decreases exponentially as the distance from the center ($r$) increases. Hence, the mass sensitivity of the nonelectroded region is much less than that of the electroded region.[3,4]

In applications of the QCM, if we only consider the effect of mass loading on the electroded region and ignore the frequency response caused by mass loading on the nonelectroded region, a large deviation between the measurements and the real value is expected. Thus, it is necessary to study the mass effect of the nonelectroded region in depth to distinguish between the frequency shift caused by the electroded region and that caused by the nonelectroded region.

The mass sensitivity distribution of QCM devices can be represented by[5]

$$S_f(r) = \frac{|A(r)|^2}{2\pi \int_0^\infty r|A(r)|^2 dr} \times C_f, \tag{2}$$

where $S_f(r)$ is the mass sensitivity function in hertz per kilogram; $A(r)$ is the particle displacement amplitude function; $r$ is the distance from the center; and $C_f$ is Sauerbrey's sensitivity constant with a value of $1.78 \times 10^{11}$ Hz·cm$^2$/kg.

The particle displacement amplitude function $A(r)$ in Eq. (2) is the solution of the following particle displacement amplitude equation

$$r^2\frac{\partial^2 A}{\partial r^2} + r\frac{\partial A}{\partial r} + \frac{k^2 r^2}{N}A = 0, \tag{3}$$

where $N$ is a constant for an AT-cut quartz crystal. According to the constants for AT-cut quartz crystal material, $N$ =2.0443.[6]

The particle displacement amplitude in Eq. (3) is a typical Bessel's equation and its solution can be written as

$$A = \begin{cases} C_1 J_0\left(\frac{k_E}{\sqrt{N}}r\right) & |r| \le m, \\ C_2 K_0\left(\frac{k_U}{\sqrt{N}}r\right) & m \le |r| < \infty, \end{cases} \tag{4}$$

where $J_0$ and $K_0$ are Bessel's functions of the first kind with order zero and modified Bessel's functions of the second kind with order zero, respectively; $C_1$ and $C_2$ are unknown amplitude constants.[7]

$$k_i^2 = \frac{\omega^2 - \omega_i^2}{c^2}, \tag{5}$$

where $i = E,U$ ($E$ is the electroded region and $U$ is the nonelectroded region); $c = \sqrt{c_{66}/\rho_q}$ is the acoustic wave velocity in the crystal ($C_{66}$ is the elastic stiffness constant and $\rho_q$ is the density of the quartz); $\omega_E$ and $\omega_U$ are the cutoff frequencies of the electroded and nonelectroded regions, respectively.

The particle displacement $A(r)$ and shear strain field are continuous at $r = m$ (where $m$ is the electrode radius). According to these boundary conditions, the boundary equations of a QCM with

the "*m–m*"-type electrode are

$$\begin{cases} A^{\mathrm{E}}|_{r=m} = A^{\mathrm{U}}|_{r=m}, \\ \dfrac{\partial A^{\mathrm{E}}}{\partial r}|_{r=m} = \dfrac{\partial A^{\mathrm{U}}}{\partial r}|_{r=m}. \end{cases} \tag{6}$$

On the basis of these boundary conditions, the ratio relation of $C_1$ and $C_2$ in eq. (4) can be determined, and the mass sensitivity function of the QCM with the "*m–m*"-type electrode $S_{\mathrm{f}}(r)$ is then determined by substituting Eq. (4) into Eq. (2).

Obviously, the measurement of the frequency shift ($\Delta f$) includes the frequency shift caused by the adsorption of mass on the electroded region as well as that caused by the adsorption of mass on the nonelectroded region. In spite of the mass sensitivity of the nonelectroded region being much less than that of the electroded region, the area of the nonelectroded region in the crystal plate is larger than that of the electrode region; thus, the frequency shift caused by the mass effect of the nonelectroded region cannot be ignored.

Through the above analysis, we see that part of the frequency shift of the QCM is caused by the mass effect of the nonelectroded region. However, what proportion of the total frequency shift ($\Delta f$) is due to the electroded or nonelectroded regions? On the basis of the assumption that the mass loading distribution is uniform within the sensing surface range of the QCM, the relationship of $\Delta f_1$ (the frequency shift caused by the adsorption of mass on the electroded region) and $\Delta f_2$ (the frequency shift caused by the adsorption of mass on the nonelectroded region) can be determined according to following equation:

$$\frac{\Delta f_1}{\Delta f_2} = \frac{\int_0^a S_{\mathrm{f}}(r)2\pi r dr}{\int_a^b S_{\mathrm{f}}(r)2\pi r dr} = \frac{\int_0^a S_{\mathrm{f}}(r) r dr}{\int_a^b S_{\mathrm{f}}(r) r dr}, \tag{7}$$

where $S_{\mathrm{f}}(r)$ is the mass sensitivity function; $a$ and $b$ are radii of the electrode and quartz plate, respectively; $r$ is the distance from the center.

Taking a gold-coated 5 MHz 3rd overtone AT-cut QCM resonator as an example, such a resonator is widely employed in high-precision measurements of minute mass changes.[8] The diameter and thickness of the round gold electrode are 10 mm (radius $a$ = 5 mm) and 1000 Å, respectively. The diameter of the 5 MHz 3rd overtone AT-cut quartz plate is 25.4 mm (radius $b$ = 12.7 mm). Then, according to Eq. (2), the profile of the mass sensitivity distribution can be obtained as shown in Fig. 1.

As expected, the mass sensitivity distribution of the gold-coated 5 MHz 3rd overtone AT-cut QCM resonator is an approximate Gaussian curve. The electroded region (solid line in Fig. 1) has a higher mass sensitivity than the nonelectroded region (dashed line in Fig. 1). The highest sensitivity point appears at the center of the electrode ($r$ = 0), and then decreases exponentially as the distance from the center ($r$) increases.

The neglect of the mass effect of the nonelectroded region of QCM greatly impacts the accuracy and practical of QCM when it is used to measure ultra-micromass, and the new method presented here can help researchers process experimental data more reasonably and accurately.

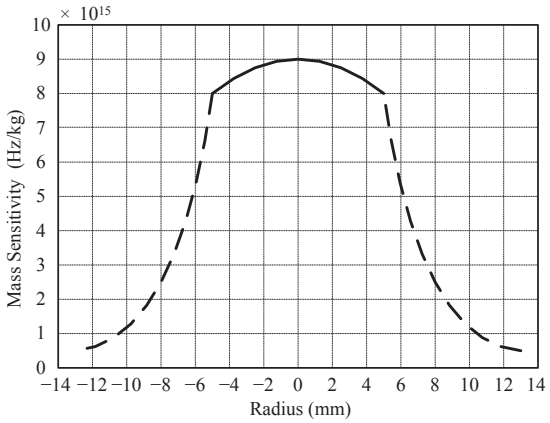


Fig. 1. Mass sensitivity distribution of gold-coated 5MHz 3rd overtone AT-cut QCM resonator. The dashed line represents the nonelectroded region ($5 < |r| < 12.7$), and the solid line represents the electroded region ($|r| < 5$).

## 2. Materials and Methods

For the gold-coated 5 MHz 3rd overtone AT-cut QCM resonator, the radii of the gold electrode (a) and quartz plate (b) were 5 and 12.7 mm, respectively. On the basis of the assumption that the mass loading distribution is uniform within the range of the sensing surface of the QCM, $\Delta f_1/\Delta f_2 = 0.7121$ was then determined using Eq. (7). The frequency shift caused by the adsorption of mass on the nonelectroded region ($\Delta f_2$) was even larger than that caused by the adsorption of mass on the electroded region ($\Delta f_1$); thus, ignoring the mass effect of the nonelectroded region caused a large deviation between the measurements and the real value.

The mass effect of the nonelectroded region has also been demonstrated by the experimental results in Ref. 8. Lee *et al*. generated highly charged airborne Vaccinia viruses in a gas mixture of air and $CO_2$ using an electrospray aerosol generator from a virus suspension.[8] The generated airborne viruses were then neutralized by a Polonium-210 source, resulting in charge-equilibrated bioaerosols. These viruses were transported into the QCM chamber and adsorbed onto a gold-coated 5 MHz 3rd overtone AT-cut quartz crystal, resulting in $\Delta f = 12$ Hz frequency shifts. Figure 2 shows a schematic of the overall experimental setup consisting of an electrospray aerosol generator and a QCM.

## 3. Results and Discussion

As an independent verification, the viruses on the QCM chip were counted by fluorescence microscopy, and the number of viruses in the electroded region of the QCM surface was $21.1 \times 10^6$ viruses. The mass of a single virus is approximately 9 fg.[9,10] Therefore, the adhered virus mass in the electroded region was calculated and denoted as $\Delta m = 189.9$ ng. By substituting $\Delta m$ into Eq. (1), the calculated frequency shift $\Delta f_1$ was approximately 4.55 Hz (reference value). We can see that the experimental result was two times larger than the reference value obtained from the independent verification experiment. Lee *et al*. did not give a reasonable explanation for this large deviation.

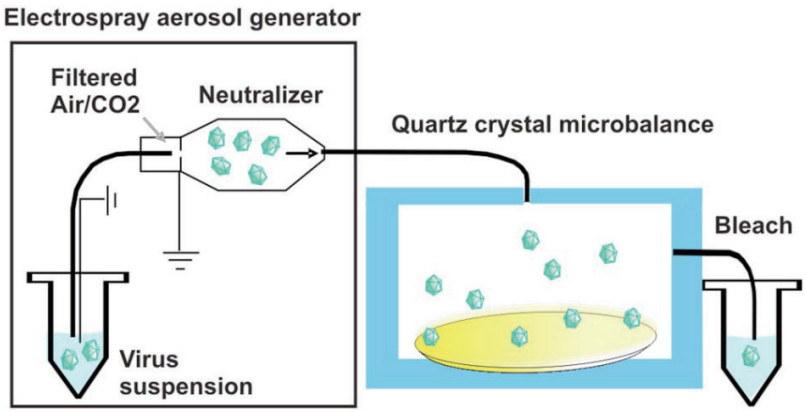


Fig. 2. (Color online) Schematic of airborne virus detection system consisting of electrospray aerosol generator and QCM.

Table 1
Uncorrected values vs corrected values.

| | $\Delta f$ (Hz) | $\Delta f_2$ (Hz) | $\Delta f_1$ (Hz) | Error (%) |
|---|---|---|---|---|
| Uncorrected values | 12 | 0 | 12 | 164 |
| Corrected values | 12 | 7.01 | 4.99 | 9.7 |

However, after considering the mass effect of the nonelectroded region, it is clear that the frequency shift $\Delta f$ consists of $\Delta f_1$ (the frequency shift caused by the adsorption of virus particles on the electroded area) and $\Delta f_2$ (the frequency shift caused by the adsorption of virus particles on the nonelectroded area). The frequency shifts observed in the experiment were $\Delta f = 12$ Hz. By the analysis described, $\Delta f_1$ can be determined from $\Delta f_1 = (\Delta f \times 0.7121)/(1 + 0.7121) = 4.99$ Hz, and $\Delta f_2 = 7.01$ Hz can be determined as well. Both are very close to the theoretical value.

Apparently, as can be seen in Table 1, the correction of the mass effect of the nonelectroded region reduced the errors between the experimental values and the reference values from 164 to 9.7%. It is clear from the experimental result that the mass effect of the nonelectroded region cannot be ignored.

## 4. Conclusions

In conclusion, the sensing surface of the QCM includes electroded and nonelectroded regions. In spite of the mass sensitivity of the unelectroded region being much less than the mass sensitivity of the electroded region, the area of the nonelectroded region is much larger than that of the electroded region; thus, the frequency shift caused by the mass effect of the nonelectroded region cannot be ignored. In this paper, we present a method based on the integral of the mass sensitivity function to distinguish between the frequency shift caused by the electroded region and the frequency shift caused by the nonelectroded region. Finally, we verify the feasibility of the correction method from the data processing results of an airborne Vaccinia virus testing experiment

using a QCM. Note that, although the rectifying formula Eq. (7) is applied to the QCM with the "*m*–*m*"-type electrode only, analysis methods based on the integral of the mass sensitivity function like Eq. (7) can still be applied to any type of QCM.

## References

1 S. M. Knudsen, J. Lee, A. D. Ellington, and C. A. Savran: J. Am. Chem. Soc. **127** (2005) 2022.
2 G. Sauerbrey: Z. Phys. **155** (1959) 206.
3 J. M. Saint Surin: United States Patent No. 8215171 (2012).
4 F. Josse, Y. Lee, S. J. Martin, and R. W. Cernosek: Anal. Chem. **70** (1996) 321.
5 J. Y. Gao, X. H. Huang, and Y. Wang: IEEE Trans. UFFC **60** (2013) 2031.
6 F. Josse, Y. Lee, S. J. Martin, and R. W. Cernosek: Anal. Chem. **2** (1998) 237.
7 S. K. R. S. Sankaranarayanan, R. Singh, and V. Bhethanabotla: IEEE Sensors Conference (IEEE, Kona, 2010) pp. 1883–1886.
8 J. Lee, J. Jang, D. Akin, C. A. Savran, and R. Bashir: Appl. Phys. Lett. **93** (2008) 013901.
9 L. Johnson, A. K. Gupta, A. Ghafoor, D. Akin, and R. Bashir: Sens. Actuators, B **115** (2006) 189.
10 A. Gupta, D. Akin, and R. Bashir: Appl. Phys. Lett. **84** (2004) 1976.